

Properties of polyethylene-polypropylene blends

Part 1 *Thermal swelling and mechanical characterization of extruded unoriented specimens*

R. GRECO, G. MUCCIARIELLO, G. RAGOSTA, E. MARTUSCELLI
*Laboratorio di Ricerche su Tecnologia dei Polimeri e Reologia, Via Toiano 2,
Arco Felice, Napoli, Italy*

High-density polyethylene (PE)—isotactic polypropylene (PP) blends have been characterized by a number of techniques such as wide-angle X-ray scattering, differential scanning calorimetry, pycnometry, swelling in *n*-hexane and finally stress-strain tensile elongation. All the measurements have been performed on cylindrical shaped specimens, obtained directly by extrusion. The specimens show a complete random orientation of the crystallites of both the components. No co-crystallization phenomenon are observed. The melting point of both PE and PP decreases slightly with increasing concentration of the second component. The fractional crystallinity of PE decreases and that of PP increases with respect to the corresponding homopolymer values with increase in the concentration of the companion polyolefin. Such an effect is related to morphological kinetic effects and to different rates of crystallization of the two components, during the non-isothermal crystallization process following extrusion. Young's modulus, E is proportional to the overall fractional crystallinity. The ultimate properties show a synergistic effect due to the strong interactions between the crystallites and their tie molecules of the two PE and PP distinct phases. Finally, it is to be remarked that the results obtained in this paper, especially with respect to the ultimate properties, are quite different from those reported by other authors. This can be attributed to the different processing conditions used for obtaining the present blend specimens. Such conditions are certainly very important in determining particular blend morphologies which will determine in turn the properties of the analysed samples.

1. Introduction

By blending two or more polymers having different molecular characteristics, materials with improved end-use properties can be obtained [1-3]. One way of characterizing binary blends is to start with studies of the physical state of each of the components individually at room temperature [3] and try to forecast the performance of the composite from the knowledge of the properties of the single constituents. Of the possible arrangements, many can be found in commercial polymers already on the market.

In previous works, blends of atactic polystyrene

(glassy at room temperature) and a series of polyolefins (semicrystalline and rubbery in their amorphous regions) have been investigated [4, 5], in order to arrive at some generalizations about a class of blends consisting of an amorphous glassy and a semicrystalline component. In the present work thermal, mechanical and swelling measurements of blends of high-density polyethylene and isotactic polypropylene are studied by a large number of techniques with the above objective, but with the difference that in this case both polymers are semicrystalline in nature.

The rheology of the mixing and the applications

of such blends have been extensively described recently by Plochocki [6]. Specifically, triangular diagrams (including as a third component a low-density polyethylene) have been studied with respect to their mechanical properties by Robertson and Paul [7] and Deanin and Sansone [8]. However, in both cases the starting polymers were insufficiently characterized as also was the blend behaviour. The latter was also not sufficiently correlated with fundamental parameters such as crystallinity and morphology. Consequently, by implication, their studies seem to attribute the observed mechanical behaviour mainly to the chemical nature of the examined polymers.

In the present paper which is part of a more general study on the properties of binary blends with at least one crystallizable component [4, 5, 9], PE and PP polymers, characterized by RAPRA, were blended and further analysed with respect to their crystallinity content, to their crystallite and overall phase orientation by different techniques. Therefore, the main goal of this series of papers is to try to relate the observed behaviour to the morphology of the sample directly obtained by a given extrusion process.

2. Experimental details

2.1. Materials

The polymers used in the present work are: high-density polyethylene (PE) ($\bar{M}_w = 166\,000$; $\bar{M}_n = 10\,200$; $\bar{M}_w/\bar{M}_n = 16$; M.F.I. = 3.7 g/10 min; $\rho = 0.96\text{ g cm}^{-3}$); isotactic polypropylene (PP) ($\bar{M}_w = 307\,000$; $\bar{M}_n = 15\,600$; $\bar{M}_w/\bar{M}_n = 20$; M.F.I. = 3.9 g/10 min; $\rho = 0.906\text{ g cm}^{-3}$) both kindly provided by RAPRA (standards HDPE 1 and PP1 respectively). The polymers were used as-received.

2.2. Blend preparation

Polymeric blends were obtained by melt mixing the pelletized components (typically 10 mm^3 pellet) at 180°C in a laboratory extruder (CSI max mixing-extruder model CS-194 manufactured by Instron Scientific Instruments Inc). The standard procedure is described elsewhere [4]. The full composition range of the PE-PP blends was surveyed the samples having the following weight percentages:

PE	0	10	30	50	70	90	100
PP	100	90	70	50	30	10	0

2.3. Methods

A Perkin Elmer model DSC-2 differential scanning calorimeter was used to determine the melting points, the enthalpy of fusion of the two semi-crystalline components, and the crystallization isotherms. All the measurements, on sample weights ranging from 4 to 8 mg, were made at a scanning speed of $20^\circ\text{C min}^{-1}$. The melting temperatures and the enthalpies of fusion were derived from the position of the maxima and from the melting peak areas, respectively. Calibration of the apparatus was made by a series of standards: benzile (m.p. 95.0°C), sulphonal (m.p. 128°C) *p*-nitro-aniline (m.p. 147.5°C), indium (m.p. 156°C). Wide-angle X-ray patterns of the extruded filaments were recorded photographically by means of a flat camera using $\text{CuK}\alpha$ Ni-filtered radiation. Gravimetric, volumetric and axial swelling measurements in *n*-hexane were also performed on the same samples.

Density measurements by picnometry were also made on the specimens: first as obtained by the extruder, then after equilibrium swelling in *n*-hexane and finally on the same samples dried under vacuum. Finally, stress-strain curves of the filaments in tensile mode at room temperature were obtained by means of an Instron machine (table model 1122) at a constant cross-head speed for all the samples of 5 mm/min. Since the samples were directly obtained by extrusion they were not dumb-bell shaped. Therefore, to avoid slippage in the clamps, scotch tape fabric was wound around the ends of the cylindrical specimens before clamping them. Marks were also made on the samples to check this. All the measurements where slippage was detected were, of course, discarded.

From the stress-strain curves the following parameters on the average value based on about eight measurements were calculated; Young's modulus [from the initial slope $(d\sigma/d\epsilon)_{\epsilon=0}$]; yield strength and elongation [from the maximum of the curve, where $(d\sigma/d\epsilon) = 0$]; strength and elongation at break.

3. Results and discussion

3.1. Thermal behaviour

Wide-angle X-ray diffraction patterns showed random orientation of the crystallites in the extruded specimens of pure polymers as well as in their blends. This isotropy of the crystalline regions is probably due to the fact that only a

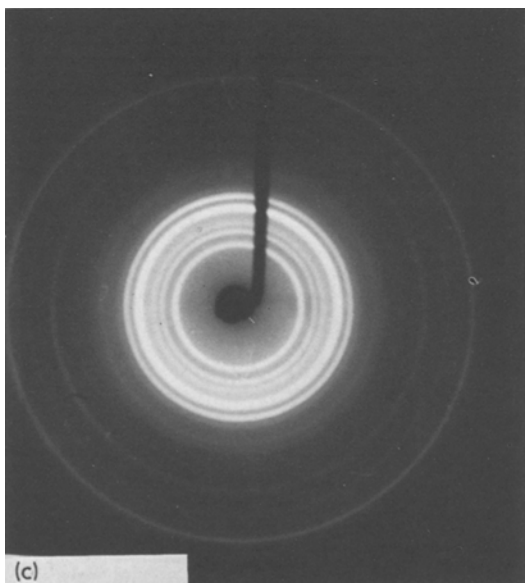
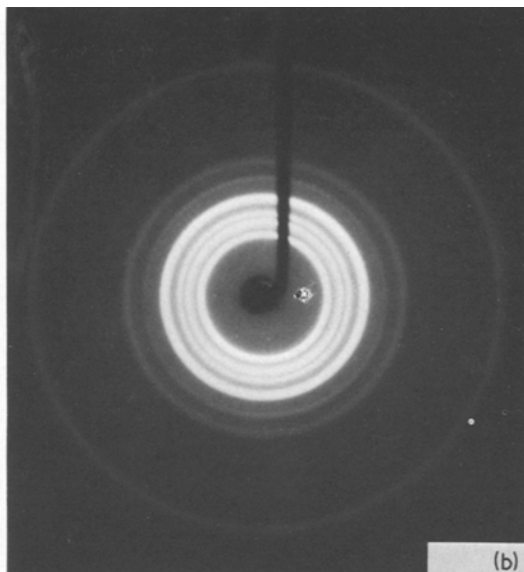
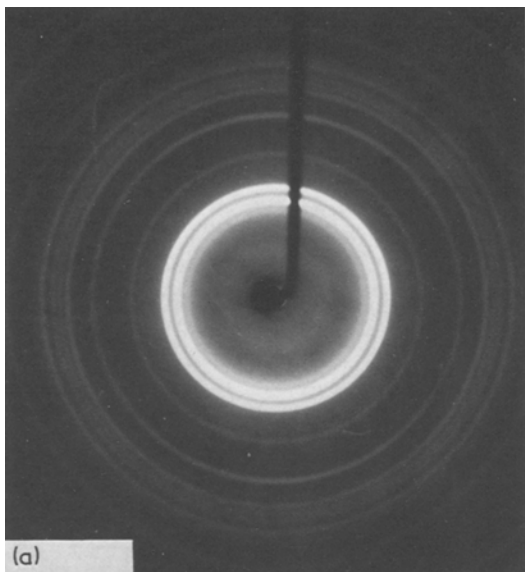


Figure 1 Wide-angle X-ray diffraction patterns: (a) pure PE, (b) pure PP, (c) 50 PP % blend.

small difference existed between the rate of extrusion of the filaments and that of the take-up system [4]. Furthermore, wide-angle X-ray diffraction patterns of the blends corresponded to a simple superposition of the photographs of the single components (Fig. 1). The intensity of the diffraction effects due to the crystalline regions is proportional to the weight ratio of the two polymers in the blends. Therefore no co-crystallization occurs in the blend during its cooling outside the extruder. The melting point, T_m , and the fractional crystallinity of PE for the extruded samples (circles) as a function of PP percentage

is shown in Fig. 2. T_m decreases linearly, whereas X_c seems to show a slight minimum for a value of the PP percentage of about 50%. Analogous plots of T_m and X_c are reported for PP as a function of PP content in Fig. 3. In addition, in this case T_m decreases linearly, whereas X_c remains constant up to a 50% PP value and then increases with increasing PE content.

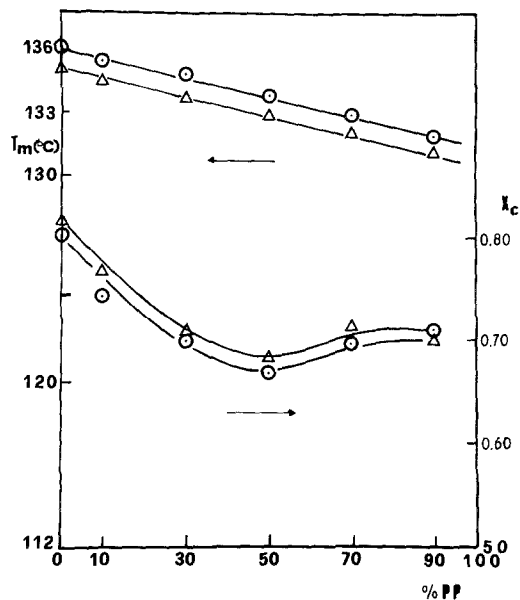


Figure 2 Melting point, T_m , and fractional crystallinity, X_c , of PE in the blends as a function of PP content.

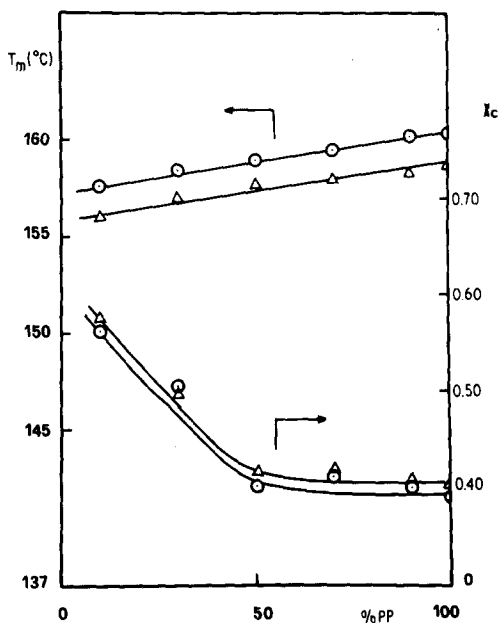


Figure 3 Melting point and fractional crystallinity, X_c , of PP in the blends as a function PP content.

The values of T_m and X_c relative to a second cycle of fusion (triangles) are also reported in Figs. 1 and 2. The procedure after the first fusion was as follows. The sample was kept at a temperature higher than the melting points of PE and PP (190°C) for 10 min, then it was crystallized by cooling it down to room temperature at a scanning rate of $20^\circ\text{C min}^{-1}$. The data of the second cycle, except for small differences in the absolute values, show analogous behaviour when compared with the first heating cycle data. Such a result is probably due to a slightly different thermal crystallization history between the first cooling cycle (after extrusion) and the second one, obtained by DSC.

It should be noted that the blends, thus crystallized, show a unique crystallization exotherm, even though the rate of crystallization of PP and PE is very different especially at low undercoolings [9]. Fusion of the blends, however, still shows two distinct melting endotherms relative to the PE and PP phases which crystallize separately. This result, which would be expected on the basis of the different molecular structure of PE and PP, is also confirmed by the wide-angle X-ray diffraction patterns, already shown in Fig. 1, where the characteristic rings of PE and PP are clearly distinguishable. Therefore, as observed by other authors [10, 11] even in the case of low- and high-density PE mixtures [12, 13], no co-crystallization is possible between two different polyolefins and

hence the blend consists of two crystalline phases and at least one amorphous phase. Furthermore, since no data are available from the literature [6, 7] to assess the compatibility of PE and PP in the molten state, the system is certainly even more complex. Therefore, if the two components are mainly incompatible, the melting depression of each component of the blends can be tentatively explained as being due to the following effects:

(1) the kinetic effect of one solid phase which may obstruct or make irregular the growth of the lamellar crystallites of the spherulites of the other phase;

(2) thermal perturbations due to different rates of crystallization between PE and PP [9].

The X_c behaviour at low PP concentrations, particularly the decrease of PE and the increase of PP with increasing content of the other component, may be mainly due to effect 2. In fact, the PP spherulites, which crystallize before PE, are surrounded by a PE melted matrix. Hence, when the PE crystallizes, the PP spherulites absorb part of the heat of crystallization of PE. This will increase the degree of crystallinity; however, this should not increase the perfection and/or the thickness of the crystals as this would raise the melting point which is not observed. In the meantime such a phenomenon may alter the radial temperature distribution of the filament compared to that in pure PE. The same arguments may also be considered to explain the decrease of PE fractional crystallinity with increasing PP content. At higher PP concentrations, where the crystallinities of PP and PE are nearly constant, the effect on X_c can instead be attributed mainly to effect 1, since the matrix is now essentially PP which has already crystallized. In the case of a small degree of compatibility between amorphous PE and PP, that one cannot exclude absolutely in principle, the Flory-Huggins [14] approach could also be added to explain the T_m depression. Such limited compatibility could also affect the degree of crystallinity of the components obtained during cooling.

3.2. Swelling behaviour

The gravimetric sorption in *n*-hexane at 40°C , $(W - W_0/W_0) 100$, and the corresponding axial elongation, $(L - L_0/L_0) 100\%$, relative to the initial weight W_0 and to the initial length of the dry filaments, were calculated on the swollen samples. Of such parameters only the first is shown to be a function of time in Fig. 4.

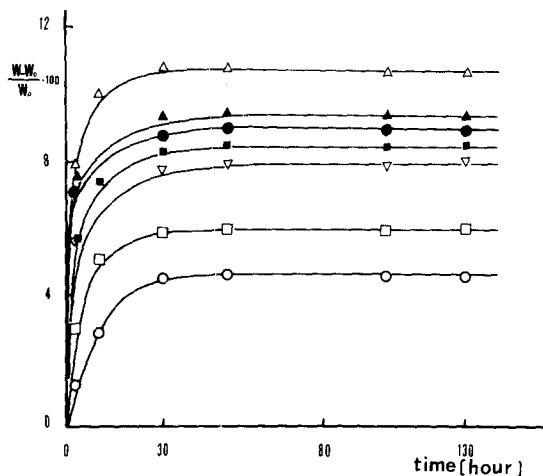


Figure 4 Relative gravimetric sorption $(W - W_0/W_0) \times 100$ as a function of time at various blend composition: Δ 100% PP; \blacktriangle 90% PP; \bullet 70% PP; \blacksquare 50% PP; ∇ 30% PP; \square 10% PP; \circ 0% PP.

The volumetric and axial equilibrium values, reached after about 10 h, and calculated from plots like those shown in Fig. 4, and from density measurements made on the swollen samples, are reported as a function of PP% in Fig. 5. Both increase with increasing PP content. The same data are also reported as a function of total amorphous fraction in Fig. 6. Such a fraction has been calculated as $(1 - X_c^t)$, where X_c^t is the overall crystallinity fraction of the blends.

$\Delta V/V_0$ increases linearly, whereas $\Delta L/L_0$ also increases but with a trend less than linear. The numerical values of $\Delta V/V_0$, $(1 - X_c^t)$, $(\Delta V/V_0)/(1 - X_c^t)$, are also reported as function of PP content (first column) in columns 2 to 4 of Table I. On inspection it is evident that PE amorphous regions absorb more than the corresponding PP zones. Such a result is somewhat surprising since the PE, having a higher crystallinity content than PP, should have a much more constraining structure than the corresponding PP one. However, PE seems to show a much stronger chemical affinity for *n*-hexane or, on the other

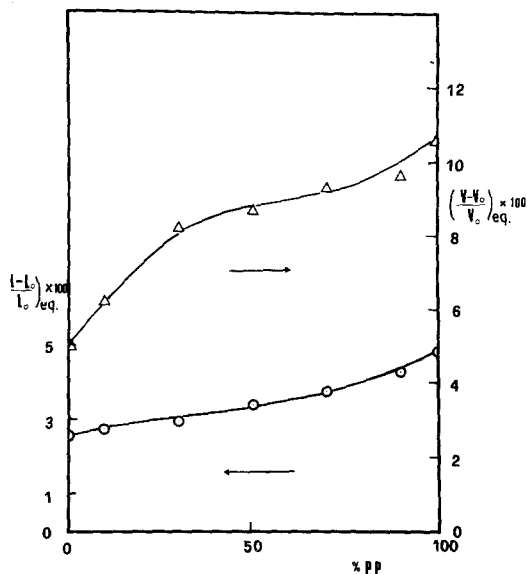


Figure 5 Equilibrium axial swelling $(L - L_0/L_0)_{eq}$ (left-hand vertical axis) and equilibrium volumetric swelling $(V - V_0/V_0)_{eq}$ (right-hand vertical axis) as a function of PP percentage.

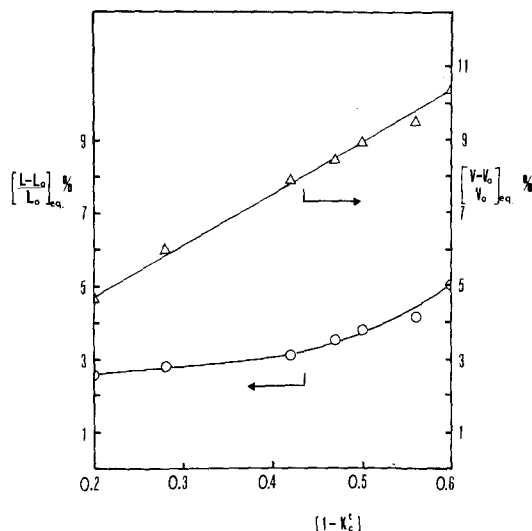


Figure 6 Equilibrium axial swelling $(L - L_0/L_0)_{eq}$ (left-hand vertical axis) and equilibrium volumetric swelling $(V - V_0/V_0)_{eq}$ (right-hand vertical axis) as a function of total amorphous fraction, $(1 - X_c^t)$.

TABLE I Absorption data in *n*-hexane for extruded samples

PP (%)	$(\Delta V/V_0)_{eq}$	$(1 - X_c^t)$	$(\Delta V/V_0)/(1 - X_c^t)$	$(L/L_0)/(V/V_0)^3$
100	0.107	0.63	1.70×10^{-1}	1.017
90	0.097	0.57	1.73×10^{-1}	1.010
70	0.091	0.50	1.80×10^{-1}	1.006
50	0.087	0.47	1.85×10^{-1}	1.005
30	0.082	0.42	1.95×10^{-1}	1.001
10	0.063	0.28	2.25×10^{-1}	1.007
0	0.048	0.20	2.40×10^{-1}	1.010

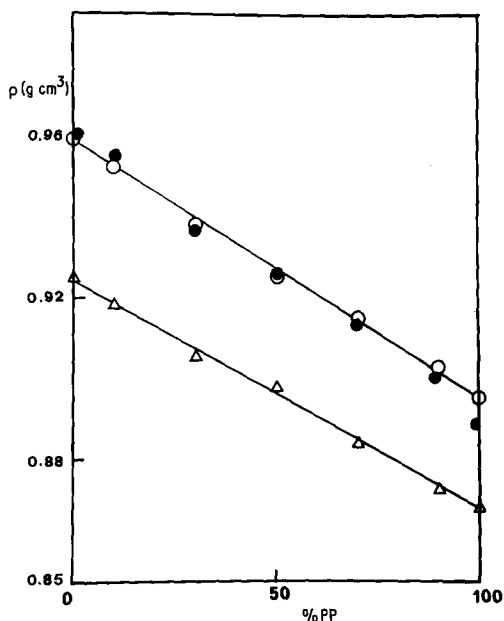


Figure 7 Density values as a function of PP percentage for the following specimens: after extrusion (○); calculated from Equations 1 and 2 (●); at equilibrium swelling (△).

hand, seems to have a morphology with a higher absorbing power than PP.

In the same table (column 5) the ratio $[(L/L_0)/(V/V_0)^{1/3}]$ is shown, which can be taken as a measure of the macroscopic isotropy of the specimens. Since such a parameter is equal to 1, over the entire composition range, this result indicates an isotropic structure of the overall extruded samples. In fact, the swelling phenomenon can be thought of as a three-dimensional mechanical expansion due to solvent adsorption into the polymeric material. Density measurements of dry (○) and equilibrium swelling specimens (△) as a function of blend composition are reported in Fig. 7. The density decreases linearly with increasing PP content in both cases.

Also shown in Fig. 7 are the density values (○) of the blends calculated according to the following relationship:

$$\rho_{\text{blend}} = W_{\text{PE}}\rho_{\text{PE}} + W_{\text{PP}}\rho_{\text{PP}} \quad (1)$$

where W_{PE} , W_{PP} are the weight fractions and ρ_{PE} , ρ_{PP} are the densities of the pure components, calculated in turn by the equation:

$$(\rho)_{\text{PE,PP}} = \left(\frac{\rho_c \rho_a}{\rho_c(1 - X_c) + X_c \rho_a} \right)_{\text{PE,PP}} \quad (2)$$

in which ρ_a , ρ_c are the densities of the amorphous

and of the crystalline regions of each polyolefin respectively, and X_c their fractional crystallinity (for PE $\rho_c = 1.000 \text{ g cm}^{-3}$ and $\rho_a = 0.855 \text{ g cm}^{-3}$, for PP $\rho_c = 0.940 \text{ g cm}^{-3}$ and $\rho_a = 0.852 \text{ g cm}^{-3}$).

The data derived from Equations 1 and 2, using the DSC values for calculating X_c , are in very good agreement with the experimental densities. Such a result could be taken as evidence for incompatibility of PE and PP in the amorphous regions. It is to be noticed, however, that the densities of the amorphous regions of the two components are too close to allow such a conclusion. The density values of the samples first swollen to equilibrium and then dried under vacuum, are not shown in Fig. 7 for sake of clarity, since they are substantially the same as those of the original extruded samples. Such a result reveals that there is no variation in the density, i.e. for selective extrusion of low molecular weight fractions of the material, during the swelling experiments.

3.3. Mechanical behaviour

The mechanical behaviour of the extruded samples is shown in Fig. 8 where typical stress-strain curves for blends of different PP contents are reported. The initial slope of such curves is by definition the Young's modulus, E , whose linear behaviour as a function of PP content is reported in Fig. 9. The overall fractional crystallinity X_c of the blends, obtained by summing the crystalline amounts of PP and PE, is also shown in Fig. 9 (right-hand vertical axis). E and X_c^t are two straight lines, therefore E is directly proportional to X_c^t . This is a very reasonable result since presumably the morphology is very similar (spherulitic) for each component in the blend over the entire composition range and is not altered by the effect of the small deformations involved in the beginning of the deformation. Successively at higher deformation values the material yields, changing its morphology from a spherulitic to a fibrous structure. We see from Fig. 8 that in the yield range the curves for blends with PP content higher than 50% lie above those for the pure components. This is more conspicuous in Fig. 10 where the yield stress σ_y and the elongation at yield ϵ_y are reported as a function of PP content. At low PP concentration both the curves are almost coincident with the two straight lines connecting the values of the pure components.

At concentrations higher than about 25% PP content, the curves start to increase more than

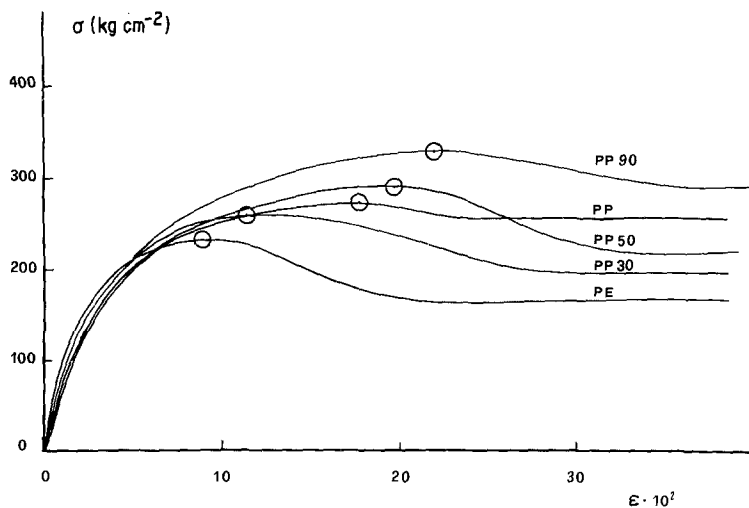


Figure 8 Typical stress-strain curves for different PP percentage blends as indicated; circles on the curves indicate yield points.

linearly, reaching a pronounced maximum at about 80% PP. For PP-rich blends such a result shows a marked reinforcing effect on the PE component, whose effect is to delay the neck formation and hence to give, yield values higher than those corresponding to the pure components. In other words, the presence of small quantities of PE in a PP matrix seems to decrease the plasticity of the material, whereas small amounts of PP do not provide any reinforcement in PE-rich blends. The same features have already been observed by some of the authors [15] in a previous work concerning the mechanical behaviour of blends of two different molecular weight fractions of poly(ethylene oxide). In that case the more

crystalline fraction (of lower molecular weight) acted as a reinforcing agent on blends rich in the more plastic component (having higher molecular weight).

The ultimate strength, σ_u , and the deformation at break, ϵ_u , as a function of PP content are reported in Fig. 11. No elongation at break values are shown in Fig. 11 for pure PE and PP, since in this case the neck propagated along the whole length of the specimens. Therefore, reliable values for σ_u in the case of such non-dumb-bell shaped samples could only be obtained by cutting their necked portions and winding up the ends of such fibers to suitable clamps.

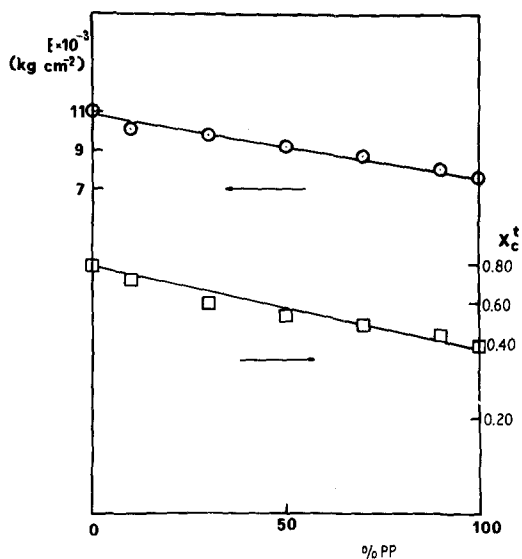


Figure 9 Young's moduli, E , and overall fractional crystallinity, X_c^t (right-hand vertical axis) as a function of PP percentage.

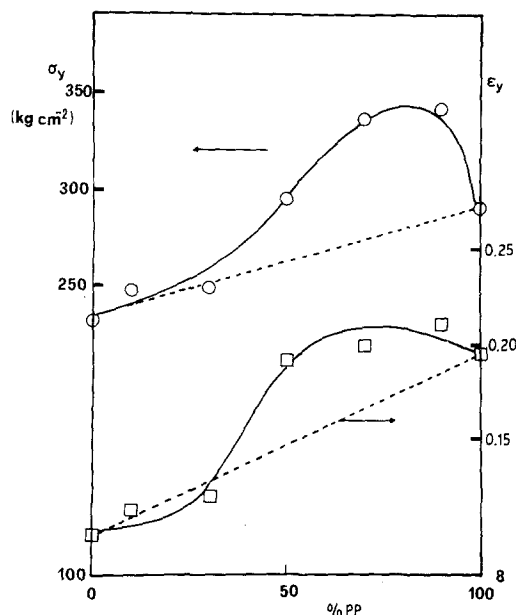


Figure 10 Yield strength, σ_y , and elongation at yield, ϵ_y , as a function of PP content.

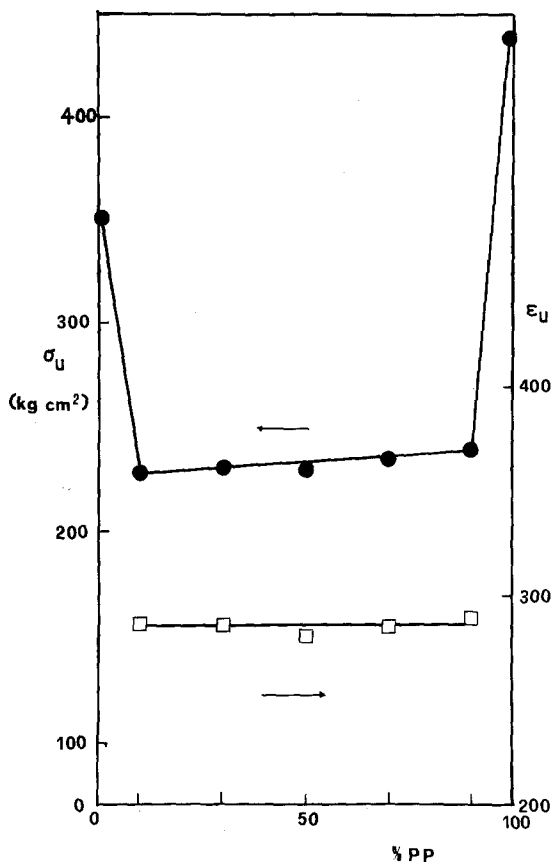


Figure 11 Ultimate strength σ_u (●) and elongation at break, ϵ_u (□) (right-hand vertical axis) as a function of PP content.

The blends show a sharp drop in σ_u with respect to the values of the pure components remaining constant over the entire range of composition thereafter. Such a feature is also present for ϵ_u . In fact, for pure PE and PP, the neck propagated along the whole length of the specimens, showing a plastic behaviour much stronger than for blends, even though no absolute values were detectable for pure components.

Such a behaviour is probably due to the interactions occurring between the crystallites of the two polymers and their connecting tie molecules. Therefore, the cold drawing and hence the morphology changes in the necked portions of the samples are more and more hampered until the specimens break. Such an interaction is also evidenced by the mechanical behaviour in the yield portion of the stress-strain curves when such morphological changes start to occur, as already shown in Fig. 10.

4. Conclusions

In conclusion, the extruded specimens of PE-PP blends show isotropic behaviour, according to the wide-angle X-ray scattering patterns and the swelling behaviour. Furthermore, the blends obtained are shown to consist of at least three or four distinct phases. In fact, no co-crystallization phenomena were detected, and no information on the compatibility between amorphous PE and PP could be obtained. Therefore at least two crystalline phases and one amorphous phase (in the case of compatible amorphous components) or two distinct amorphous phases (for incompatible amorphous regions) are present in the blends.

By mixing PE and PP, some of the properties (such as T_m , ρ , E) show an additive trend of the two, whereas others show strong non-linear interactions (σ_y , ϵ_y , and σ_u , ϵ_u). It should be remarked, however, that such features cannot be attributed only to the chemical nature of both PE and PP. In fact, other authors [7, 8] using other processing conditions for making their samples, find different mechanical behaviour.

From these observations one can conclude that the properties of blends of two crystallizable components are strongly dependent upon processing conditions. In fact, such conditions probably influence the overall morphology of the materials, i.e. spherulite dimensions, structure of interphase regions and nature of amorphous regions, which in turn will determine the properties of the blends.

References

1. D. DEANIN, A. DEANIN and T. SJOBLOM, in "Recent Advances in Polymer Blend, Grafts and Blocks", edited by H. Sperling (Plenum Press, New York, 1974).
2. J. A. MASON and L. H. SPERLING, in "Polymer Blends and Composites" (Plenum Press, New York, 1976).
3. R. GRECO and E. MARTUSCELLI, "Leghe Polimeriche" *La Chimica & l'Industria* **61**(4) (1979) 298.
4. R. GRECO, H. B. HOPFENBERG, E. MARTUSCELLI, G. RAGOSTA and G. DEMMA, *Polymer Eng. Sci.* **18** (1978) 654.
5. M. COSTAGLIOLA, R. GRECO, E. MARTUSCELLI and G. RAGOSTA, *J. Mater. Sci.* **14** (1979) p. 1152.
6. A. P. PLOCHOCKI, "Polymer Blends", edited by D. R. Paul and S. Newman (Academic Press, New York, 1978).
7. R. E. ROBERTSON and D. R. PAUL, *J. Appl. Polymer Sci.* **17** (1973) 2579.
8. R. D. DEANIN and M. F. SANSONE, *Polymer Symp.* **19**(1) (1978) 211.
9. E. MARTUSCELLI, M. PRACELLA, M. AVELLA,

- R. GRECO and G. RAGOSTA, *Macromol. Chem.*, to be published.
10. D. V. FILBERT, V. P. MURAVEVA and YU. A. GLAZKOVSKII, *Karbolsepnnye Volokna* **82** (1966) 140.
 11. L. BOHN, *Rubber Chem. Technol.* **41** (1968) 495.
 12. B. B. STAFFORD, *J. Appl. Polymer Sci.* **9** (1965) 729.
 13. B. H. CLAMPITT, *J. Polymer Sci.* **3A** (1965) 671.
 14. P. J. FLORY, *J. Chem. Phys.* **10** (1942) 51.
 15. J. BRANDRUP and E. H. IMMERGUT, "Polymer Handbook", 2nd edn. (John Wiley and Sons, New York, 1975).
 16. S. CIMMINO, R. GRECO, E. MARTUSCELLI, L. NICOLAIS and C. SILVESTRE, *Polymer* **19** (1978) 1079.

Received 26 April and accepted 11 September 1979.